

Phase evolution in solution deposited Pb-deficient PLZT thin films

Krishna Nittala · Geoff L. Brennecka ·
Bruce A. Tuttle · Jacob L. Jones

Received: 10 August 2010/Accepted: 3 November 2010/Published online: 17 November 2010
© Springer Science+Business Media, LLC 2010

Abstract Initial crystallization of Pb-deficient, lanthanum modified lead zirconate titanate (PLZT) layers followed by post-crystallization phase conversion can be used to obtain high quality PLZT thin films. However, phase evolution in Pb-deficient PLZT thin films is not well understood. To characterize phase evolution in these films, we developed a new *in situ*, high-temperature X-ray diffraction (XRD) measurement approach for slow heating rates. The well-characterized Pb-excess PLZT composition was used for comparison and to validate the new XRD setup described herein. During crystallization of Pb-deficient thin films, a Pb-rich/La-poor perovskite phase and Pb-poor/La-rich fluorite phase were observed to form simultaneously. The fluorite phase was observed to partially transform into a secondary perovskite phase at higher temperatures. The results obtained are discussed in view of the current understanding of phase evolution in these materials. The details of the new *in situ* XRD technique are also presented.

Introduction

Lead zirconate titanate (PZT)-based thin films are used for integrated capacitors, ferroelectric memory, and piezoelectric actuators [1–4]. Solution deposition is an attractive route for fabrication of PZT-based ferroelectric thin films

due to its low cost and good stoichiometric control. In solution deposition of thin films, initially the solution is deposited on the substrate and dried to form an amorphous film. The amorphous film is crystallized by heating it to a high temperature. Doping of PZT thin films with donor dopants, such as La^{3+} , is routinely done to improve the dielectric properties of PZT and decrease the electrical conductivity of the thin films by compensating for cation vacancies. Cation vacancies are formed in undoped PZT due to the volatilization of Pb in the form of PbO .

The presence of secondary non-ferroelectric phases, such as fluorite [5], and the film–substrate interaction [6] are the primary causes for decrease in properties of Pb-based thin films. Complete crystallization of the perovskite phase can be hampered by Pb loss, and typically results in the observation of a Pb-deficient non-ferroelectric fluorite phase at the surface of the film. A common approach to deal with the fluorite problem has been to formulate solutions that are superstoichiometric in Pb precursor to compensate for PbO volatility during heat treatment. However, the presence of excess Pb species appears to promote greater interaction between the film and the substrate leading to a decrease in properties and reduced control over Pb stoichiometry within the film [6]. Moreover, fluorite phase is often still observed on the top surface in Pb-excess PZT-based thin films [5].

To address the limitations of the standard fabrication route, Brennecka et al. [7] recently developed a new route for making ultra thin films using solution deposition. The uniqueness of this approach is to deliberately start with a Pb-deficient solution, which is meant to decrease the film–substrate interaction. The resulting multi-phase (stoichiometric perovskite + Pb-deficient fluorite) films are converted to single-phase perovskite through a post crystallization heat treatment under a PbO overcoat. Using

K. Nittala · J. L. Jones (✉)
Department of Materials Science and Engineering,
University of Florida, Gainesville, FL 32611, USA
e-mail: jjones@mse.ufl.edu

G. L. Brennecka · B. A. Tuttle
Materials Science and Engineering Center, Sandia National
Laboratories, Albuquerque, NM, USA

this approach, high quality ultra thin films of PZT can be made. This study was devised to compare this new fabrication approach with the standard Pb-excess technique in terms of phase evolution and associated film–substrate interactions.

Few studies have focused explicitly on phase evolution of Pb-deficient PZT-based materials. Polli et al. [8] carried out a comprehensive study of phase formation in sol–gel-derived PZT powders. They observed that the fluorite phase is the stable phase on crystallizing the powders at 500 °C. A metastable perovskite phase formed upon crystallizing the powders at higher temperatures ~600–700 °C, and finally a perovskite single phase was formed on crystallizing at ~800 °C. While this study provides insight into the crystallization behavior of PZT-based materials, phase evolution is expected to be significantly different in thin films due to the presence of the film–substrate interface and the unique sample geometries. For example, Pt_xPb , a metastable intermetallic phase, has been observed during crystallization of Pb-rich thin films deposited on Pt bottom electrodes [9–11]. This transient intermetallic phase is suggested to affect phase and texture evolution in these thin films.

X-ray diffraction (XRD) is a standard technique for characterizing phase evolution in solution deposited thin films. Most studies using XRD for characterization of phase evolution in solution deposited thin films have been done using quenched samples or samples that were intermittently heated [12, 13]. Sample to sample variability and the dynamic nature of phase evolution may introduce significant error in these methods. Phase evolution in solution deposited thin films is a dynamic process affected by the heat treatment history and the processing conditions. Hence, it is desirable to characterize phase evolution in thin films *in situ* during crystallization.

In an earlier study, Wilkinson et al. [14] studied phase evolution in sol–gel derived powders *in situ* by collecting the diffraction pattern over a limited 2θ range on a Bragg–Brentano type diffractometer during crystallization. Multiple diffraction patterns were measured to map the evolution of phases with time. The kinetics of phase evolution were studied by tracking the integrated peak intensity of the (200) peak with respect to heat treatment time. It was observed that the fluorite phase always preceded the formation of perovskite in PZT and lead zirconate powders. No fluorite phase was observed in lead titanate powders. Although this method provided valuable information about phase evolution in sol–gel derived powders, it cannot be directly applied to solution deposited thin films because the movement of the detector over the required 2θ range makes this technique inherently slow. Phase evolution in solution deposited thin films is faster in comparison to powders [15] and hence, it is desirable to develop a technique which allows for rapid characterization of phases during crystallization of thin films.

With the above motivation, a new diffraction based technique was developed to study phase evolution in solution deposited thin films *in situ* during crystallization. Briefly, a curved position sensitive (CPS) detector is used to simultaneously collect diffraction data over a wide 2θ range while the sample is heated to the crystallization temperature. The use of a CPS detector allows for rapid acquisition of diffraction data and characterization of phase evolution in the thin film.

Experimental

La-doped PZT thin films (PLZT) were deposited from solution on single crystal Si substrates with a sputtered Pt layer (Pt(170 nm)//Ti(40 nm)// SiO_2 (400 nm)//Si). For this study the La, Zr, and Ti contents were all maintained constant with a ratio of 6/52.2/46.3 (corresponding to a stoichiometric PLZT composition of 6/53/47 with B-site compensation for the donor doping associated with La addition). From this base composition, 20% of the Pb content was either added to the batch calculations (PLZT 6/53/47 + 20% Pb, referred to for the remainder of this study simply as Pb-excess) or subtracted from the batch calculations (PLZT 6/53/47–20% Pb, referred to as Pb-deficient). Solutions for spin coating were prepared by the inverted mixing order (IMO) method developed by Assink and Schwartz [16]. The B-site precursors (zirconium butoxide and titanium isopropoxide) were first weighed and mixed in glacial acetic acid. After mixing, the A-site precursors (lead acetate and lanthanum acetate) were added to the solution. The solution was mixed at ~90 °C to dissolve the Pb(IV) acetate into the solution. After dissolution of lead acetate, the solution was cooled and diluted to the required molarity using acetic acid and methanol. The solution thus prepared was spin coated onto platinized silicon wafers at 3000 rpm. Three layers were spin coated and the films were pyrolyzed between each spin coating step. Specific details of the solution deposition process can be found elsewhere [17], but for this study, the films were pyrolyzed at 300 °C after each spin-deposited layer and were crystallized during heating within a furnace mounted on a diffractometer to allow *in situ* characterization of the crystallization process. The thin films were ~350 nm thick after crystallization.

A CPS detector was used to measure diffraction patterns *in situ* while the thin films were crystallized in the furnace during heating. The CPS detector is a one dimensional detector which simultaneously measures the diffraction pattern over a wide 2θ range. This allows for rapid acquisition of the diffraction data. The furnace used in the experiment is equipped with a Kapton sleeve to allow for the transmission of the incident X-rays to the sample and

the diffracted X-rays to the detector. All the films were crystallized in air by continuously heating from room temperature to a final temperature in the range of 600–650 °C at a rate of 5 °C/min. A heating rate of 5 °C/min was used to minimize the uncertainty in the temperature. Patterns were each measured sequentially for an acquisition time of 60 s. Each pattern therefore represents the measurement of the time-averaged structure across a 5 °C window of temperature. The slow heating rate also allowed for collection of considerable diffraction intensities from the different phases formed during crystallization. To compensate for the possibility of greater PbO volatilization due to the slower heating rate, for Pb-excess films, 20% excess Pb precursor was added to the starting solution. After crystallization, the samples were cooled to room temperature at the same rate (5 °C/min). Diffraction patterns were measured during both heating and cooling.

Certain peaks in the measured XRD patterns were fit to profile shape functions to extract quantitative information. In peak fitting, the background of the entire diffraction pattern from $2\theta = 20^\circ$ to 80° was fit first using an eighth order polynomial function. The peaks were then each individually fit to a Pearson VII-type function using the curve fitting tool box in Matlab©. The Pearson VII function was modified to include diffracted intensities from both K_{z1} and K_{z2} of the incident X-ray beam; the position between the components was constrained by their difference in wavelength and the peak shape parameters of each component were set equal. Lattice parameters were calculated after correcting for the shift in 2θ positions due to sample displacement by thermal expansion [18].

Grazing incidence X-ray diffraction (GIXRD) patterns were measured on the crystallized thin films using a Philips X'pert diffractometer. Diffraction patterns were measured at different incidence angles to probe different depths of the thin film.

Results

The first crystalline phase observed during crystallization of Pb-excess thin films is a Pt_xPb intermetallic phase. The evolution of the diffraction pattern of the Pb-excess thin film during crystallization is shown in Fig. 1a. The changes in the phases formed during the crystallization of Pb-excess thin films are shown in Fig. 3a. Based on previous reports on the Pt_xPb intermetallic, it was assumed that any intermetallic formed would be crystalline and will be observed in the diffraction pattern [9]. The maximum amount of Pt_xPb is observed to be present at $T = 430 \pm 2.5$ °C. The intermetallic phase eventually disappears as the film is ramped to higher temperatures and is no longer seen after $T = 471 \pm 2.5$ °C. A fluorite phase appears at

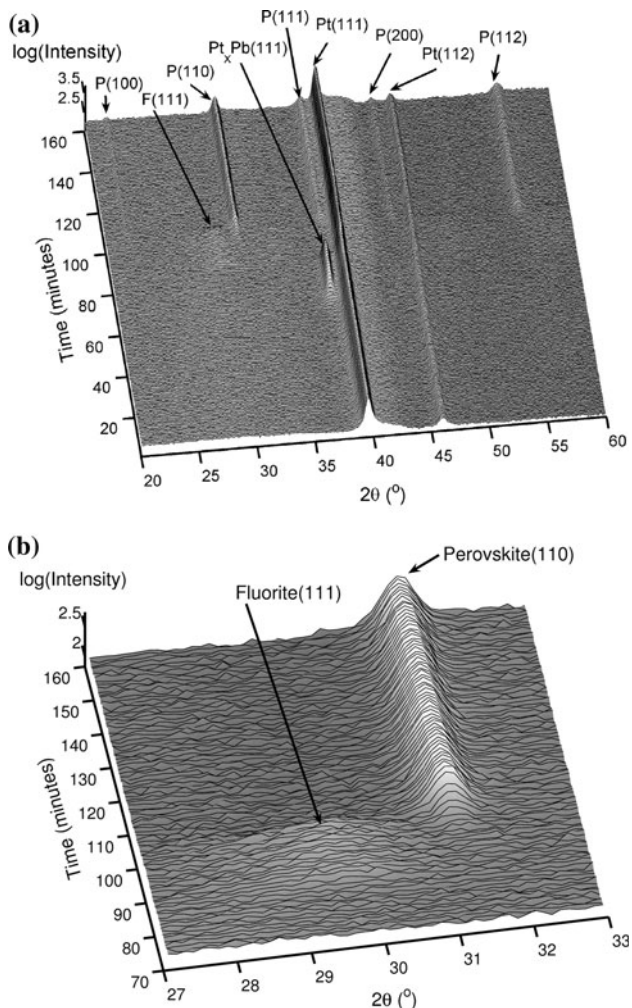


Fig. 1 Phase evolution in Pb-excess thin films. **a** Contour plot showing phase evolution during gradual heating. **b** A limited 2θ and time plot showing the disappearance of the fluorite (111) peak and the appearance of the perovskite (110) peak is shown. Perovskite peaks are indexed assuming a pseudocubic perovskite structure

$T = 440 \pm 2.5$ °C and reaches maximum diffraction intensity at $T = 471 \pm 2.5$ °C. Finally, the perovskite phase appears at $T = 511 \pm 2.5$ °C and reaches a maximum by $T = 552 \pm 2.5$ °C. The appearance of the perovskite phase and the disappearance of the fluorite phase seem to be correlated. Figure 1b is a contour plot on a limited 2θ and time region showing the disappearance of the fluorite phase and the appearance of the perovskite.

In Pb-deficient thin films, a perovskite and fluorite type phase appear together at $T = 506 \pm 2.5$ °C. The evolution of the diffraction patterns during crystallization is shown in Fig. 2a. The evolution of the phases during crystallization is shown in Fig. 3b. The amount of fluorite observed reaches a maximum at $T = 553 \pm 2.5$ °C. The perovskite reaches a maximum at $T = 580 \pm 2.5$ °C. Thereafter, on holding at $T = 600$ °C, an additional distinct perovskite phase is observed. To distinguish from the perovskite phase

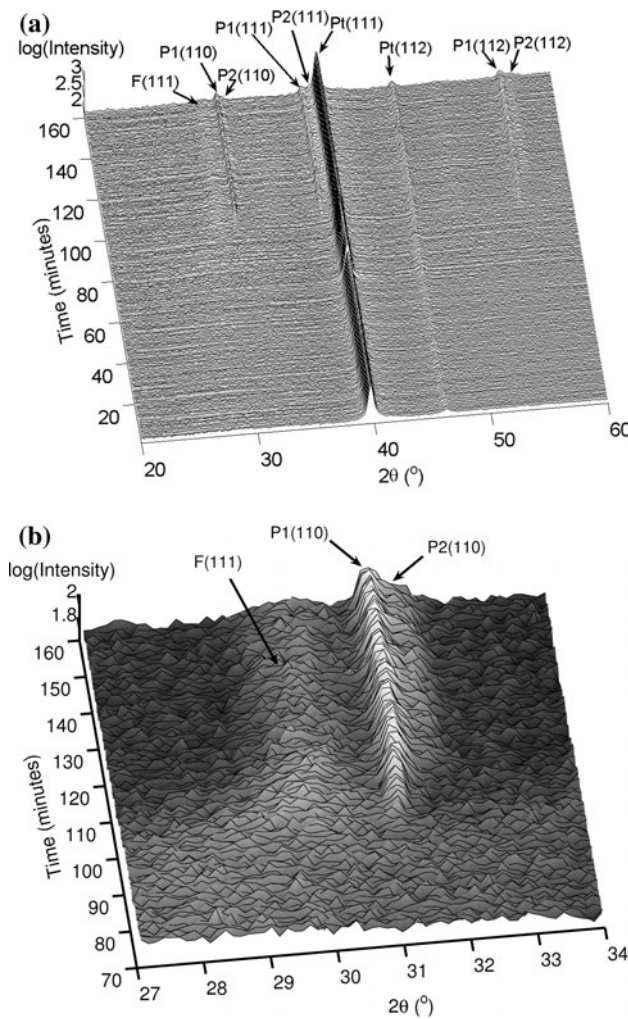


Fig. 2 **a** Phase evolution in Pb-deficient films with gradual increase in temperature. **b** A limited 2θ and time plot showing the fluorite (111) and perovskite (110) peaks shows the gradual evolution of the fluorite and perovskite peaks with time and temperature. P1 and P2 are used to designate perovskite-1 and -2, respectively

formed in the Pb-excess thin films, the first perovskite phase formed in the Pb-deficient thin film is designated as perovskite-1 and the secondary perovskite phase formed later in processing time is called perovskite-2 for the remainder of this article. There is a decrease in the observed fluorite phase content from the point where the perovskite-2 phase is observed. At the end of the heat treatment the fluorite type, perovskite-1 and -2 phases are all observed to be present.

The lattice parameters of the perovskite phases formed in Pb-excess and -deficient thin films are listed in Table 1. The lattice parameters of the perovskite phases were calculated at 500 °C from the diffraction patterns measured during the cooling of the sample (not shown) after crystallization. Since this temperature is above the Curie temperature of the perovskite phases, the crystal structure was assumed to be pseudocubic.

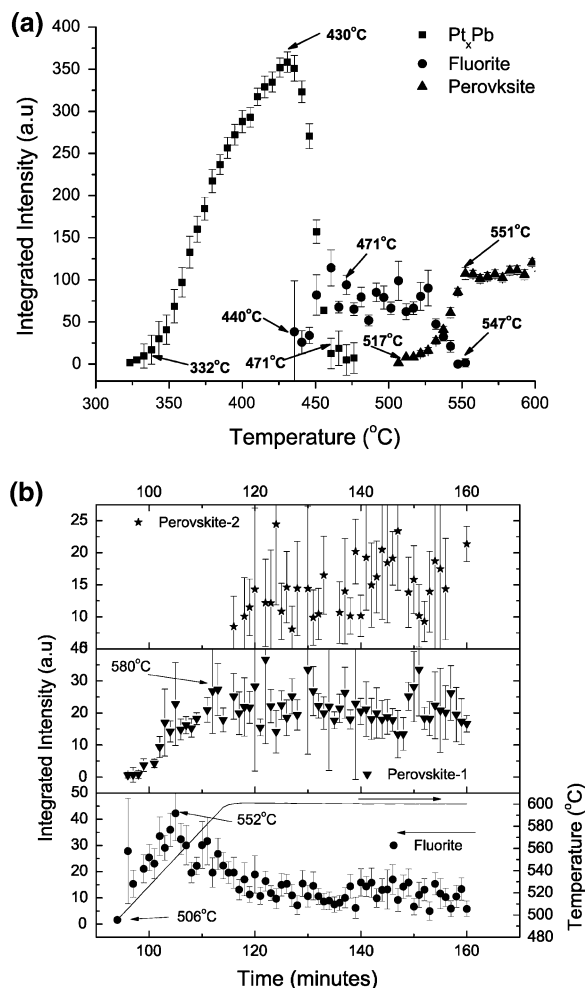


Fig. 3 Phase evolution during crystallization of **a** PLZT + 20% excess PbO thin film and **b** PLZT + 20% deficient thin film. The solid line in the plot shows the variation of temperature with time. Perovskite-2 phase is formed after reaching 600 °C and on subsequent holding. All temperatures shown in the figures have an error of ± 2.5 °C. Error bars shown correspond to 3σ

Table 1 Lattice parameters of the different perovskite phases formed in the thin films investigated

Film composition	Phase	Lattice parameter (Å)
Pb-excess	Perovskite	4.08
Pb-deficient	Perovskite 1	4.08
Pb-deficient	Perovskite 2	4.02

Perovskite-1 and -2 refer to the perovskite phases formed in Pb-deficient thin films. Lattice parameters were calculated at ~ 500 °C assuming a pseudocubic perovskite crystal structure

Discussion

In Pb-excess thin films (Fig. 3a), the temperature range in which the Pt_xPb intermetallic phase is observed is consistent with that reported by Chen et al. [11] (400–700 °C)

and Huang et al. [13] (330 °C). From the observed diffraction peaks of the Pt_xPb intermetallic, the structure corresponds to the Pt_3Pb phase reported by Huang et al. [13]. The temperature at which the perovskite phase is observed to form is consistent with that observed by Kwok and Desu [19]. The observed sequence of phases formed during crystallization in the Pb-excess thin films is found to be consistent with previous reports on crystallization of PZT thin films [19–21].

Pt_xPb is not observed to form in the Pb-deficient thin films (Fig. 2a), indicating that this reaction between the electrode and the thin films is reduced with a decrease in the Pb content in the thin film. Several possible reasons for the absence of Pt_xPb in Pb-deficient thin films can be hypothesized. First, due to the lower amount of total PbO present in the film, the rate at which Pt_xPb is formed may decrease. However, the rate at which oxygen diffuses from the atmosphere to the film–substrate interface remains unchanged. Pt_xPb is unstable in the presence of oxygen and decomposes to PbO and platinum. Due to the decreased rate of formation of Pt_xPb in Pb-deficient films, the rate of oxygen diffusion from the atmosphere may be sufficient to destabilize any Pt_xPb formed. Second, it is possible that the amorphous phase consists of a nanocrystalline fluorite phase [22] which is not detected by X-ray diffraction. This nanocrystalline fluorite phase could control the availability of free PbO , leading to very little availability of PbO for reduction and subsequent formation of Pt_xPb at the interface.

Polli et al. [8] observed that the formation of the fluorite and perovskite phases is delayed with a decrease in the Pb content in the powders. The trend in fluorite phase formation observed in this study ($T \sim 440 \pm 5$ °C for Pb-excess and $T \sim 506 \pm 5$ °C for Pb-deficient) agrees with the trend reported by Polli et al. However, the perovskite phase formation observed in this work does not agree with the trend reported for sol–gel derived powders in Polli et al. The perovskite phases were observed to form at similar temperatures ($T \sim 506 \pm 5$ °C for Pb-deficient and $T \sim 517 \pm 5$ °C for Pb-excess) for the thin films. Moreover, the fluorite phase and the perovskite-1 phase form at the same time and temperature in the Pb-deficient thin film. These discrepancies with earlier results are explained as follows. Nucleation of the perovskite phase in thin films preferentially occurs heterogeneously at the film–electrode interface. As crystallization of solution derived PZT is nucleation dependent [23], the temperature at which the perovskite phase is first observed is determined by the stabilization of the perovskite nuclei by the interface. Although the growth rate of the perovskite nuclei has been observed to be affected by the Pb content in the films, the nucleation rates were found to not significantly differ with Pb content (Pb-excess = 0–20%) in PZT thin films [24].

The observation of the formation of perovskite phases in both Pb-excess and -deficient films at similar temperatures implies that the nucleation rates could be similar for both Pb-excess and -deficient films used in this study.

During crystallization, the perovskite phase in Pb-excess thin films is observed to reach its maximum intensity by $T \sim 550$ °C (10 min), while the perovskite-1 phase in Pb-deficient films reaches a maximum by around $T \sim 580$ °C (15 min). Deviation from ABO_3 stoichiometry in PZT is expected to destabilize the perovskite phase. However, in this study a Pb-excess in the solution is observed to help to crystallize the film faster than starting with a Pb-deficient solution. Similar behavior was observed in solution derived powders [8] and sol–gel deposited PZT layers on LaAlO_3 [24] substrates. Based on EXAFS studies by Sengupta et al. [25], Polli et al. [8] hypothesized that excess Pb acts as a network modifier that assists in rearranging the atoms for the formation of the required perovskite phase. This is a possible explanation for the faster crystallization of the perovskite phase in Pb-excess thin films. It should also be noted that the starting solutions nominally varied from stoichiometry by the same magnitudes, though in different directions. Pb loss during processing may bring the initially Pb-rich films closer to stoichiometry while pushing the Pb-deficient films further from stoichiometry.

Parish et al. [26] characterized the final phases obtained after crystallization of Pb-deficient PLZT (12/70/30) thin films. Chemical segregation was observed in thin films which had been crystallized at 650 °C for 30 min using a 50 °C/min furnace ramp rate. The thin films were found to contain a perovskite and a fluorite phase. The perovskite phase was found to be Pb-rich and La-deficient relative to the nominal composition and was formed closer to the electrode than the fluorite phase, which was Pb-deficient, La-rich, and present near the top surface of the film. In the thin films in this study, apart from the fluorite and perovskite-1 phases, an additional perovskite phase (perovskite-2) is observed. Substitution of La^{3+} for Pb^{2+} in PZT causes a decrease in unit cell volume and lattice parameter [27]. The diffraction peaks of this La-substituted perovskite phase would be observed at higher 2θ values relative to the perovskite-1 phase formed initially. Hence, it is proposed that the perovskite-2 formed in the Pb-deficient films crystallized from the remnant Pb-poor and La-rich fluorite phase at longer times or slower ramp rates.

Segregation in PZT thin films due to easier nucleation of lead titanate (PT) rich solid solutions at the interface has been reported to occur during crystallization [28]. PT rich compositions have a smaller unit cell volume compared to lead zirconate (PZ) rich compositions [29]. Early crystallization of a PT rich phase during in situ crystallization would show in the diffraction pattern as peaks at slightly higher 2θ values compared to the later-formed PZ rich

phase. However, during crystallization of the Pb-deficient thin film, diffraction peaks from the earlier formed perovskite-1 phase are observed at lower 2θ values compared to the later-formed perovskite-2 phase. Hence, the perovskite-1 unit cell is larger than that of perovskite-2 (Table 1). Since it is unlikely that a PZ rich composition would crystallize first, therefore perovskite-1 and -2 phases are possibly not due to PT rich and PZ rich regions segregating in the thin film.

Due to the specific geometry of the X-ray diffractometer used in this study, the poles of the diffracting planes are not perpendicular to the sample surface. Hence, texture relationships cannot be directly interpreted from the diffraction data. However, it can be qualitatively observed that $(00l)$ type peaks are present in Pb-excess films (Fig. 1a) and are not present in Pb-deficient films (Fig. 2a). This is consistent with previous reports suggesting Pb-excess is a necessary condition for the formation of $(00l)$ oriented grains [20]. GIXRD was undertaken to selectively probe the structure of the thin film. By varying the angle of incidence of the incoming X-ray beam, different depths of the thin film were probed. The change observed in the diffraction pattern with change in angle of incidence is shown in Fig. 4a. It is observed that the perovskite-1 phase is present in greater quantities closer to the interface of the film with the bottom electrode, while the perovskite-2 phase and the fluorite phase are present closer to the surface (Fig. 4b). This observation agrees well with the results of Parish et al. [26]. A possible explanation for the proximity of both the fluorite and the perovskite-2 phase to the surface is that the perovskite-2 phase is formed from the segregated fluorite phase.

Formation of a secondary perovskite phase was not observed in earlier studies on Pb-deficient PLZT thin films made by similar methods [7, 26, 30]. The perovskite-2 phase was observed to form in this study even though the final temperatures to which the thin films were heated were comparable or lower. The longer time available for crystallization in these experiments could be the reason the perovskite-2 phase was observed. In this study, the thin films were heated using a ramp rate of $5\text{ }^{\circ}\text{C}/\text{min}$, while Brennecka et al. [7] and Parish et al. [26, 30] crystallized the thin films using a heating rate of $50\text{ }^{\circ}\text{C}/\text{min}$ or by inserting the sample in a furnace pre-heated to $700\text{ }^{\circ}\text{C}$. The slower ramp rate used in this work ($5\text{ }^{\circ}\text{C}/\text{min}$) may provide additional time for PbO volatility as well as cation diffusion and segregation.

Conclusions

Phase evolution in solution deposited PLZT thin films was investigated by using a newly developed in situ diffraction

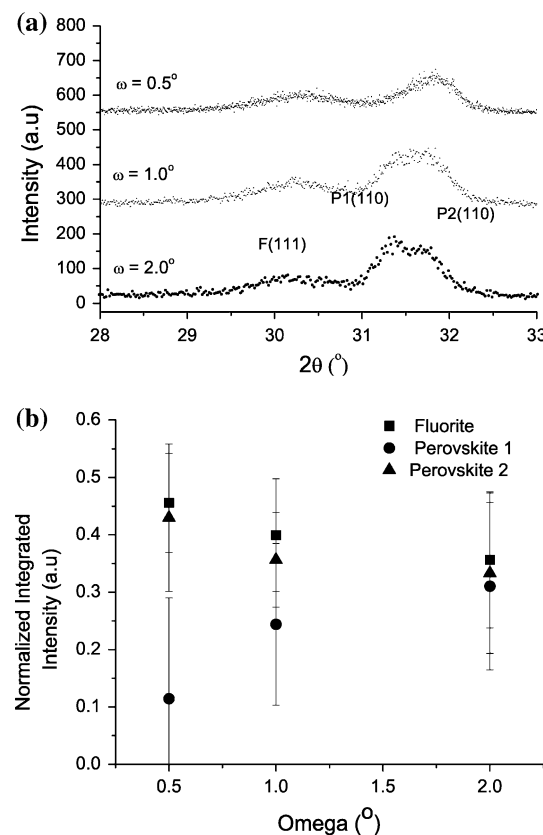


Fig. 4 a GIXRD plots for the Pb-deficient thin films at different angles of incidence ($\omega = 0.5^\circ$, 1.0° , and 2.0°). b Normalized integrated intensities of the different phases obtained with increasing X-ray incidence angles. Fluorite and perovskite-2 phases are present in greater quantities near the surface of the thin film

technique. The observed phase evolution in Pb-excess PLZT thin films was consistent with the results reported on the temperature of formation of Pt_xPb by other groups. For Pb-deficient PLZT thin films, the film is observed to partition into two phases: (1) a Pb-rich and La-poor perovskite phase and (2) Pb-poor/La-rich fluorite phase. The fluorite phase partially transforms to a perovskite phase at higher temperature. Moreover, Pt_xPb , an intermetallic formed due to interaction between the thin film and the electrode, was not observed in the Pb-deficient thin film.

It is proposed that this in situ high temperature diffraction-based technique can be used to characterize the effects of dopants, pyrolysis, and solution chemistry on phase evolution. Knowledge of how different variables affect phase evolution can help to identify strategies to decrease the crystallization temperature.

Acknowledgements This work was supported by the National Institute for NanoEngineering (NINE) and the Laboratory Directed Research and Development program at Sandia National Laboratories. Sandia National Laboratories is a multi-program laboratory operated by Sandia Corporation, a wholly owned subsidiary of Lockheed Martin Company, for the U.S. Department of Energy's

National Nuclear Security Administration under contract DE-AC04-94AL85000. JLJ acknowledges NSF for funding through award number DMR-0746902. The authors would also like to thank Dr. Valentin Craciun and MAIC at University of Florida for access to the Philips X'Pert XRD and Pat Mahoney at Sandia National Laboratories for help in preparation of samples.

References

1. Dimos D, Mueller CH (1998) *Annu Rev Mater Sci* 28:397
2. Scott JF (2007) *Science* 315:954
3. Muralt P (2000) *J Micromech Microeng* 10:136
4. Auciello O, Scott JF, Ramesh R (1998) *Phys Today* 51:22
5. Reaney IM, Brooks K, Klissurska R, Pawlaczek C, Setter N (1994) *J Am Ceram Soc* 77:1209
6. Brennecke GL, Tuttle BA (2007) *J Mater Res* 22:2868
7. Brennecke GL, Parish CM, Tuttle BA, Brewer LN, Rodriguez MA (2008) *Adv Mater* 20:1407
8. Polli AD, Lange FF, Levi CG (2000) *J Am Ceram Soc* 83:873
9. Huang Z, Zhang Q, Whatmore RW (1998) *J Mater Sci Lett* 17:1157
10. Chen SY, Chen IW (1998) *J Am Ceram Soc* 81:97
11. Chen SY, Chen IW (1994) *J Am Ceram Soc* 77:2332
12. Griswold EM, Weaver L, Sayer M, Calder ID (1995) *J Mater Res* 10:3149
13. Huang Z, Zhang Q, Whatmore RW (1999) *J Appl Phys* 85:7355
14. Wilkinson AP, Speck JS, Cheetham AK, Natarajan S, Thomas JM (1994) *Chem Mater* 6:750
15. Chen J, Udayakumar KR, Brooks KG, Cross LE (1992) *J Appl Phys* 71:4465
16. Assink RA, Schwartz RW (1993) *Chem Mater* 5:511
17. Brennecke GL, Parish CM, Tuttle BA, Brewer LN (2008) *J Mater Res* 23:176
18. Pramanick A, Omar S, Nino JC, Jones JL (2009) *J Appl Cryst* 42:490
19. Kwok CK, Desu SB (1993) *J Mater Res* 8:339
20. Chen SY, Chen IW (1994) *J Am Ceram Soc* 77:2337
21. Lakeman CDE, Xu ZK, Payne DA (1995) *J Mater Res* 10:2042
22. Norga GJ, Vasilic F, Fe L, Wouters DJ, Van der Biest O (2003) *J Mater Res* 18:1232
23. Kwok CK, Desu SB (1994) *J Mater Res* 9:1728
24. Jacobs RN, Salamanca-Riba L (2003) *J Mater Res* 18:1405
25. Sengupta SS, Ma L, Adler DL, Payne DA (1995) *J Mater Res* 10:1345
26. Parish CM, Brennecke GL, Tuttle BA, Brewer LN (2008) *J Mater Res* 23:2944
27. Breval E, Wang C, Dougherty JP, Gachigi KW (2005) *J Am Ceram Soc* 88:437
28. Calame F, Muralt P (2007) *Appl Phys Lett* 90:162901
29. Jaffe B, Cook WR, Jaffe H (1971) *Piezoelectric ceramics*. Academic Press, New York
30. Parish CM, Brennecke GL, Tuttle BA, Brewer LN (2008) *J Am Ceram Soc* 91:3690